EJTAS
ISSN 2786-7447
EUROPEAN JOURNAL OF THEORETICAL AND APPLIED SCIENCES
OPEN ACCESS
PEER REVIEWED

Dissipative Non-Slip MHD Nanofluid Flow with Variable Viscousity and Thermal Conductivity in the Presence of Arrhenius Chemical Reaction

Kelvin O. Ogboru
Department of Mathematics, Federal University of Petroleum Resources, Effurun, Nigeria

Muhammad M. Lawal
Department of Mathematics, Federal University of Petroleum Resources, Effurun, Nigeria

Akindele M. Okedoye
Department of Mathematics, Federal University of Petroleum Resources, Effurun, Nigeria

Suggested Citation

Ogboru, K.O., Lawal, M.M., & Okedoye, A.M. (2024). Dissipative Non-Slip MHD Nanofluid Flow with Variable Viscousity and Thermal Conductivity in the Presence of Arrhenius Chemical Reaction. *European Journal of Theoretical and Applied Sciences, 2*(3), 592-608.
DOI: 10.59324/ejtas.2024.2(3).45

Abstract:

This research investigates the intricate dynamics of dissipative non-slip magnetohydrodynamic (MHD) nanofluid flow, characterized by variable viscosity and thermal conductivity, under the influence of an Arrhenius chemical reaction. The inclusion of the Arrhenius chemical reaction adds complexity through heat generation or absorption, impacting temperature and concentration gradients. The study is motivated by the extensive applications of nanofluids in engineering and industrial processes, where precise control of heat and mass transfer is critical. We develop a comprehensive mathematical model that incorporates the variable properties of the nanofluid, the effects of the Lorentz force due to the applied magnetic field, and the temperature-dependent reaction rates dictated by the Arrhenius equation. The formulated governing equations were non-dimensionalised to identify the flow governing parameters. Finite Element Method (FEM), grid generation, solution algorithms, and post-processing to analyse velocity, temperature, and concentration distributions were used to obtain the numerical methods to solve fluid flow problems based on the Navier-Stokes equations, involving concepts of discretization. pdsolve subpackage in Maple 2023 was used to numerically solve PDEs with specific initial and boundary conditions, incorporating the plot and display commands for graphical analysis, and the results are presented and discussed. The findings reveal that the interplay between parameters like Hartmann number, Darcy parameter, and heat generation or absorption profoundly influences flow behaviour and thermal characteristics. The reactivity parameter is crucial, dictating the rate of chemical reactions and affecting system dynamics. This research enhances understanding of the interdependencies among fluid properties, chemical reactions, and external parameters in nanofluid flows.

Keywords: *Magnetohydrodynamics, Viscosity, Thermal conductivity, Arrhenius chemical reaction, nanofluid.*

Introduction

Fluid dynamics, crucial to various engineering and scientific fields, studies the motion of liquids and gases, analysing flow patterns, forces, and environmental impacts, with applications in aerospace, civil, mechanical, and biomedical

engineering. Advancements in computational modelling and experimental methods have deepened our understanding of complex behaviours, particularly in magnetohydrodynamics (MHD), where magnetic fields interact with fluid flows, improving industrial heat transfer processes.

Magnetofluid dynamics, encompassing magnetohydrodynamics (MHD) and magnetogasdynamics (MGD), studies the interactions between magnetic fields and the flow of conductive fluids such as liquid metals and ionized gases. This field traces its origins to Oersted's 1819 discovery of the effect of electrical currents on magnetic fields and Ampere's elucidation of the magnetic field's direction relative to current flow. Modern research includes Berman's and Terrill and Thomas's work on MHD flows in industrial applications involving porous walls and pipes. Recent advancements incorporate variable fluid properties and magnetic effects on fluid flow and heat transfer, with studies by Sattar and Maleque (2005) on rotating disks, Osalusi (2007) on magnetic effects, and Singh (2003) and Ahmed et al. (2010) on free convection and mass transfer. The Soret effect's influence on flow and thermal characteristics has also been significant. Additionally, Tania and Samad (2010), Singh et al. (2012), have furthered understanding of MHD flow, radiation effects, and boundary layer behaviours in various engineering and industrial contexts.

Specific studies, such as Bulinda et al. (2020) on oscillating surfaces in MHD flow and Waini et al. (2022) on unsteady MHD hybrid ferrofluid flow, have revealed significant effects on heat transfer parameters. Nanofluids, containing nanoparticles, exhibit superior thermal conductivity, enhancing heat transfer rates as shown by Saeed et al. (2021) and Misra & Kamatam (2020). Advanced mathematical models and computational techniques like the Darcy-Forchheimer model and Homotopy analysis method have furthered insights into these complex fluids' behaviours.

Recent studies on nanofluids, which were first introduced by Choi in 1995, highlight their potential to enhance heat transfer in industrial applications. Shah et al. (2019) and Hamid et al. (2019) examined the effects of magnetohydrodynamics (MHD) and thermal radiation on Casson micropolar ferrofluid flow over stretching sheets, revealing significant impacts on temperature profiles and heat transfer. Further research by Rashidi & Nezamabad (2011) and Bahiraei & Hangi (2015) explored heat transfer under magnetic influences. The works of Sheikholeslami & Houman (2018), Dawar et al. (2018), and Sheikholeslami (2019) delved into thermal conduction and convective boundary layer flow in nanofluids, enhancing our understanding of their complex behaviours. Moreover, studies on the effects of rarefaction in microsystems, as indicated by the Knudsen number, have significant implications for nanofluid applications. Research by Khan et al. (2020) and Giri et al. (2021) on heat generation, absorption, and activation energy in nanofluids, along with investigations by Saleem et al. (2020) and Mallick et al. (2019) on Hall current effects, have provided insights into fluid flow in rotating channels and magnetic fields. Additionally, Alanazi et al. (2023) and Jamshed et al. (2022) studied the impact of MHD, heat radiation, and activation energy on micropolar nanofluid flow, finding that magnetic fields significantly influence temperature and nanoparticle distribution.

These studies underscore the broad applicability and ongoing innovation in nanofluid technology, which continues to expand across various engineering and industrial domains.

Problem Formulation

Motivated by some of the researchers mentioned above and its applications in various fields of science and technology, it is of interest to discuss and analyse the Diffusion thermos and chemical reaction effects on the free convection heat and mass transfer flow of nanofluid over a vertical plate embedded in a porous medium in the presence of radiation absorption and constant heat source under fluctuating boundary conditions. Revisiting the work of Prasad et al. (2018), the physical model of the fluid flow is

shown in Fig. I and considering the importance of pressure gradient, buoyancy, variable viscosity and thermal conductivity in the analysis of nanofluid flow. The flow is assumed to be in the x-direction which is taken along the plate and y-direction is normal to it.

A uniform external magnetic field of strength B_0 is taken to be acting along the y −direction. It is assumed that the induced magnetic field and the external electric field due to the polarization of charges are negligible. The plate and the fluid are at the same temperature T_∞ and concentration C_∞ in a stationary condition, when $t \geq 0$, the temperature and concentration at the plate fluctuate with time harmonically from a constant mean. The fluid is a water based nanofluid containing two types of nanoparticles either Cu (copper) or TiO_2 (Titanium oxide). The nanoparticles are assumed to have a uniform shape and size. Moreover, it is assumed that both the fluid phase nanoparticles are in thermal equilibrium state. Due to semi-infinite plate surface assumption, furthermore the flow variables are functions of y and time t only.

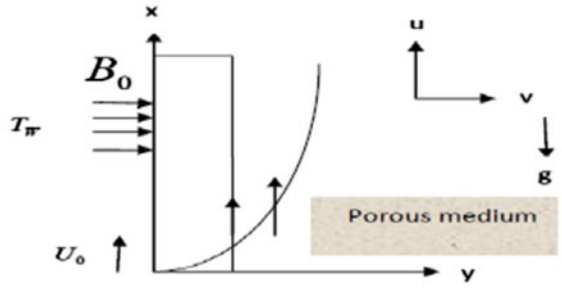

Figure 1. Schematic Diagram of the Physical Problem

Under the above boundary layer approximations, they consider the governing equations for the nanofluid flow are given by

$$\frac{\partial v}{\partial y} = 0, \tag{1}$$

$$\rho_{nf}\left(\frac{\partial u}{\partial t} + v\frac{\partial u}{\partial y}\right) = u_e\frac{du_e}{dx} + \frac{\partial}{\partial y}\left(\mu_{nf}\frac{\partial u}{\partial y}\right) - \frac{\mu_{nf}u}{K} - \sigma B_0^2 u - \frac{g(\rho\beta)_{nf}\beta_T}{\rho_{nf}}(T - T_\infty) + \frac{g(\rho\beta)_{nf}\beta_C}{\rho_{nf}}(C - C_\infty) \tag{2}$$

$$\left(\frac{\partial T}{\partial t} + v\frac{\partial T}{\partial y}\right) = \frac{\partial}{\partial y}\left(k_{nf}\frac{\partial T}{\partial y}\right) + \sigma B_0^2 u^2 + \frac{Q(T-T_\infty)}{(c_p\rho)_{nf}} + \frac{q'''}{(\rho c_p)_{hnf}} + \left(\mu_{nf}\frac{\partial u}{\partial y}\right)^2 + \frac{Dmk_T}{(\rho c_p)_{nf}C_s}\frac{\partial^2 C}{\partial y^2} + Q_1C_1A_1\left(\frac{KT}{\xi l}\right)^m e^{-\frac{E_1}{RT}} + Q_2C_2A_2\left(\frac{KT}{\xi l}\right)^m e^{-\frac{E_2}{RT}} \tag{3}$$

$$\frac{\partial C}{\partial t} + v\frac{\partial C}{\partial y} = D_B\frac{\partial^2 C}{\partial y^2} + K_r^2(C - C_\infty)\left(\frac{KT}{\xi l}\right)^m e^{-\frac{E_2}{RT}} \tag{4}$$

where u and v are the velocity components along x and y axes respectively.K_r is the Binary chemical reaction parameter, β_{nf} is the coefficient of thermal expansion of nanofluid, σ is the electric conductivity of the fluid, ρ_{nf} is the density of the nanofluid, μ_{nf} is the viscosity of the nanofluid, $(\rho C_p)_{nf}$ is the heat capacitance of the nanofluid fluid, g is the acceleration due to gravity, K is the permeability porous medium, T is the temperature of the nanofluid, Q is the temperature dependent volumetric rate of the heat source, and α_{nf} is the thermal diffusivity of the nanofluid, where ϕ is the solid volume fraction of the nanoparticles, K_{nf} and K_s are thermal conductivities of the base fluid and of the solid respectively. The thermo-physical properties of the pure fluid (water), copper and titanium which were used for code validation are given in Table 1.

The rate of heat generation is given as

$$q''' = \left(\frac{k_{nf}u_w(x)}{xv_{nf}}\right)\left[\frac{A^*(T_w - T_\infty)}{bx}u + Q_0(T - T_\infty)\right] \quad (5)$$

(A^*, Q_0) denoted the space and temperature dependent heat source/sink coefficient, respectively. Moreover, if $(A^* > 0$ and $Q_0 > 0)$ correlates to internal heat generation, while when $(A^* < 0$ and $Q_0 < 0)$ correlates to internal heat absorption.

The surface temperature and concentration of the sheet is assumed to vary by both the sheet and time, in accordance with $T_w(0,t) = T_\infty + b(1-\alpha t)^{-2}$ and $C_w(x,t) = C_\infty + b(1-\alpha t)^{-2}$ respectively. The wall temperature and concentration $T_w(0,t)$, $C_w(0,t)$ increases (reduces), if b is positive (negative) and is in proportion to x. Moreover, the amount of temperature and concentration increase (reduce) along the sheet increases with time. Here $v_w(t) = -v_0/\sqrt{(1-\alpha t)}$ at is the velocity of suction $v_0 > 0$ or blowing $v_0 < 0$. The expression for $U_w(0,t), v_w(t), C_w(0,t), \lambda(t), \kappa_r(t)$ is valid for time $t < \alpha^{-1}$.

The boundary conditions for the problem are given by

$$t < 0, u(y,t) = 0, T = T_\infty, C = C_\infty \; \forall y$$
$$t \geq 0, \begin{cases} u(y,t) = U_0, T = T_w + (T_w - T_\infty)\varepsilon e^{i\omega t}, \\ C = C_w + (C_w - C_\infty)\varepsilon e^{i\omega t} \\ u = 0, T = T_\infty, C = C_\infty \; as \; y \longrightarrow \infty \end{cases}$$

where T is the local temperature of the nanofluid and Q is the additional heat source. On the other hand, β_f and β_C are the coefficients of thermal expansion of the fluid and of the solid, respectively, ρ_f and ρ_C are the densities of the fluid and of the solid fractions, respectively, while ρ_{nf} is the viscosity of the nanofluid, α_{nf} is the thermal diffusivity of the nanofluid, and $(\rho C_P)_{nf}$ is the heat capacitance of the fluid, which are defined as (Abbasi, 2015)

$$\left.\begin{aligned} \rho_{nf} &= (1-\phi)\rho_f + \phi\rho_s \\ \alpha_{nf} &= \frac{K_{nf}}{(\rho c_p)_{nf}} \\ \mu_{nf} &= \frac{\mu_f}{(1-\emptyset)^{2.5}} \\ (\rho c_p)_{nf} &= (\rho c_p)_f(1-\phi) + \phi(\rho c_p)_s \\ (\rho\beta)_{nf} &= (\rho\beta)_f(1-\phi) + \phi(\rho\beta)_s \end{aligned}\right\} \quad (6)$$

The thermal conductivity of nanofluid of a spherical Nanoparticle (Okedoye et.al., 2023, Lawal et al. 2024a,b) is given as:

$$k_{nf} = k_f\left[\frac{k_s + 2k_f - 2\emptyset(k_f - k_s)}{k_s + k_f - \emptyset(k_f - k_s)}\right] \quad (7)$$

where f and s are the subscript of the quantities in the base fluid and nanoparticles respectively.

$$v = -v_0 \quad (8)$$

where the constant $-v_0$ represents the normal velocity at the plate which is positive suction $(v_0 > 0)$ and negative for blowing injection $(v_0 < 0)$.

Table 1. Thermo-Physical Properties of Water, Copper and Alumina

Physical properties	Titanium oxide (TiO2)	Base fluid (Water)
$C_p(JKg^{-1}k)$	686.2	4179
$\rho(kg/m^3)$	4250	997.1
$\kappa(W/mK)$	8.9538	0.613
$\rho C_p(Jkg^{-1}kkg/m^3)$		4,166,880.9
$\beta \times 10^{-5}(1/K)$	0.9	21

Rate of Heat and Mass Transfer at the Wall

The quantities of engineering interest are the local skin friction c_f, Nusselt number Nu and Sherwood number Sh. These parameters characterize the wall heat and nano mass transfer rates,

The quantities Skin friction coefficient and Nusselt number are denoted by c_f and Nu respectively and are define similar to Ometan et al. (2024) as follows:

$$c_f = \frac{\tau_w}{\rho_{nf} U_w^2}, \tag{9}$$

$$Nu = \frac{x q_w}{k_0(T_w - T_\infty)}, \tag{10}$$

$$Sh_x = \frac{x J_w}{D(C_w - C_\infty)}, \tag{11}$$

where τ_w represents the skin friction along the surface, q_w the heat flux and J_w the mass flux from the surface is respectively given as

$$\left.\begin{aligned} \tau_w &= \left[\mu_{nf} \frac{\partial u}{\partial y}\right]_{y=0}, \\ q_w &= \left[-k_{nf} \frac{\partial T}{\partial y}\right]_{y=0}, \\ J_w &= -D\left(\frac{\partial C}{\partial y}\right)_{y=0} \end{aligned}\right\} \tag{12}$$

where U_w and q_w, represents the wall shear stress and heat transfer respectively.

None-Dimensionalisation

The assumed variable plastic dynamic viscosity and thermal conductivity used for the non-Newtonian fluid are Jawali and Chamkha (2015); Gbadeyan et al. 2020

$$\left.\begin{aligned} \mu_{nf}(T) &= \mu_{nf} e^{-a^*(T-T_\infty)} \text{ and} \\ k(T) &= k_{nf} e^{-b(T-T_\infty)} \end{aligned}\right\} \tag{13}$$

Thermal conductivity varies linearly with temperature in the range of 0 to 400 F (Savvas et al. 1994 and Gbadeyan et. Al. 2020). Therefore, variable thermal conductivity is approximated as

$$\begin{aligned} k(T) &= k_{nf} e^{-b(T-T_\infty)} \\ &\approx k_{nf}\left(1 - b(T - T_\infty)\right) \end{aligned} \tag{14}$$

where μ_{nf}^* is the constant value of the coefficient of viscosity far from the plate, k_{nf}^* is the constant value of the coefficient of thermal conductivity far from the plate, a$*$ and b are the empirical constants. The constants a^* and $\mathrm{b}\ (0 < \mathrm{a}^*, \mathrm{b} << 1)$ may be positive values for fluids and negative values for gases (Jangilis et al. 2019; Gbadeyan et. Al. 2020).

We now define conveniently the following dimensionless quantities;

$$\left.\begin{aligned} x' = \frac{x}{L}, y' = \frac{y}{\delta}, v' = \frac{v}{U}\frac{L}{\delta}, V = \frac{U_1}{U_0}, u' = \frac{u}{U}, \\ \omega' = \frac{4\omega\nu}{v_0^2}, p' = \frac{p}{\rho U^2}, t' = \frac{t v_0^2}{4\nu} U' = \frac{U}{U_0}, \\ \frac{(T-T_\infty)E_a}{R_G T_\infty^2} = \theta(t,y), \frac{(C-C_\infty)}{C_w - C_\infty} = \psi(t,y) \end{aligned}\right\} \tag{15}$$

where L is the horizontal length scale, δ is the boundary layer thickness at $x = L$, which is unknown. We will obtain an estimate for it in terms of the Reynolds number $R.U$ is the flow velocity, which is aligned in the $x-$ direction parallel to the solid boundary.

Now using equation (5), (7), (8), (13) – (15) in equations (1) – (4), momentum in $x-$ and $y-$ directions, energy and species equations after dropping "primes" becomes.

$$\begin{aligned} \frac{\partial u}{\partial t} + v\frac{\partial u}{\partial y} = G + \frac{\mu_{nf}}{\mu_f}\frac{\partial}{\partial y}\left(e^{-\kappa\theta(t,y)}\frac{\partial u}{\partial y}\right) \\ -\frac{\mu_{nf}}{\mu_f}\frac{1}{K}\,u - Mu + Grt\theta(t,y) \\ +Grc\psi(t,y) = 0 \end{aligned} \tag{16}$$

$$\frac{(\rho c_p)_{nf}}{\rho_f}\left(\frac{\partial}{\partial t}\theta(t,y)+v\frac{\partial}{\partial y'}(\theta(t,y))\right)$$
$$=\frac{k_{nf}}{\mu_f}\frac{\partial}{\partial y}\left(e^{-\kappa\theta(t,y)}\frac{\partial}{\partial y}(\theta(t,y))\right)+Mu'^2$$
$$+Q_0\theta(t,y)+\left(\frac{k_{nf}}{\mu_f}\right)[A+B\theta(t,y)]$$
$$+\frac{\mu_{nf}}{\mu_f}e^{-\kappa\theta(t,y)}\left(\frac{\partial u}{\partial y}\right)^2+Due^{-\kappa\theta(t,y)}\frac{\partial^2\psi}{\partial y^2}$$
$$+(\delta_1+\delta_2)\big(1+\epsilon\theta(t,y)\big)^m e^{\frac{\theta}{1+\varepsilon\theta}} \quad (17)$$

$$\frac{\partial\psi(t,y)}{\partial t'}+v'\frac{\partial\psi(t,y)}{\partial y'}=\frac{1}{Sc}\frac{\partial^2\psi(t,y)}{\partial y'^2}$$
$$+\lambda\big(\psi(t,y)\big)\big(1+\epsilon\theta(t,y)\big)^m e^{\frac{\theta}{1+\varepsilon\theta}} \quad (18)$$

With the boundary conditions

$$t<0, u=0,\quad \theta(t,y)=1,\quad \psi(t,y)=1$$
$$t\geq 0,\begin{cases} u=\alpha,\theta=1,\psi=1\ at\ y=0\\ u=0,\theta=0,\psi=0\ as\ y\longrightarrow\infty\end{cases}$$

Numerical Solution

Computational Fluid Dynamics (CFD) is a field that uses numerical methods and algorithms to solve and analyze problems involving fluid flows, based on the Navier-Stokes equations which describe the motion of fluid substances by accounting for physical phenomena such as velocity, pressure, density, and temperature within a fluid flow. Key concepts in applying numerical solutions for our model include discretization, where continuous partial differential equations (PDEs) are transformed into discrete algebraic equations using the Finite Element Method (FEM); grid generation, where the physical domain is divided into a computational grid or mesh that can be structured or unstructured depending on the geometry; solution algorithms, which involve iterative solvers Successive Over-Relaxation (SOR), and Multigrid methods and post-processing, where tools Maple *display* command are used to visualize and analyse the flow field, providing insights into velocity distributions, temperature gradients, concentration and other flow characteristics. The 'pdsolve 'subpackage in Maple a powerful tool for solving partial differential equations (PDEs) was invoked to implement sequences of numerical codes written and executed with Maple 2023 release. The command 'pdsolve (sy11, IBC, fcns, numeric) 'is used to find numeric solutions to PDEs. Here, 'sy11'represents the system of PDEs to be solved, IBC specifies the initial and boundary conditions, and 'fcns'denotes the functions involved in the equations. The 'numeric 'option indicates that a numerical solution is sought. Incorporating *plot* code into the Maple command ensured that the graph is properly formatted and displayed using *display* command. The graphical results and tables are presented and discoursed below.

Result and Discussion

Our discussion of result on "Dissipative Non-Slip MHD Nanofluid Flow with Variable Viscosity and Thermal Conductivity in the Presence of Arrhenius Chemical Reaction" is centred on the identified flow governing parameters, As discuss below: Figure 2 display the velocity distributions in 3D. Showing the variation in velocity withing the time and spatial domain (*t, y*). From the figure, we observed that introduction of nano-particles serves as control for the fluid velocity as it lowers the magnitude of the velocity. This is required in a system where turbulence is not required and also aid prevention of loss of useful energy. Similar scenario is observed in temperature profile, Figure 3. In this figure, temperature was observed to increased rapidly close to the surface and eventually brought to a stable over time. Such situation could be likened to system over heating control mechanism. A typical example is the thermostat in cooling system of automobile engines. Once the sensor detects an excessive increase in temperature it sends a signal to the brain-box which instantaneously put cooling fan on. The scenario in chemical species is not significant as the medium for the nano - particle

is the fluid mixed desired particles to achieve the targeted aim, this is shown in Figure 4.

Velocity Distribution

The investigation of velocity distribution within nanofluid flow, influenced by magnetic fields (MHD), variable viscosity, thermal conductivity, and Arrhenius chemical reactions, reveals critical insights for system efficiency and heat transfer dynamics. Figures 5 to 7 illustrate how these factors interplay over time, showing that velocity reaches a steady state at $t \geq 6$. The introduction of nanoparticles stabilizes the velocity, reducing its magnitude as nanoparticle concentration increases, which is beneficial in applications where lower fluid velocities are required.

The pressure gradient serves as the primary driving force, with positive gradients accelerating the fluid and negative gradients decelerating it. This gradient significantly impacts the velocity profile, leading to parabolic distributions in laminar flow and affecting boundary layer thickness depending on whether the gradient is favourable or adverse.

Further analysis reveals the effects of the Hartmann number (Figure 8), which shows that increasing magnetic damping suppresses velocity gradients, leading to a flatter profile and thinner

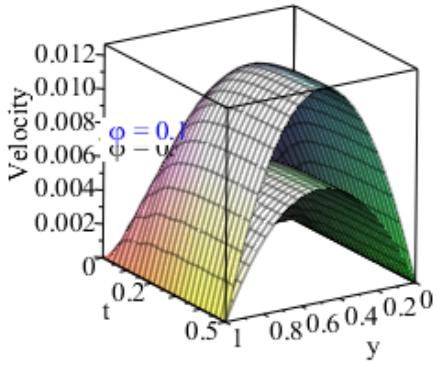

Figure 2. 3-Dimensional Display of Velocity profile for $\varphi = 0$ and $\varphi = 0.1$

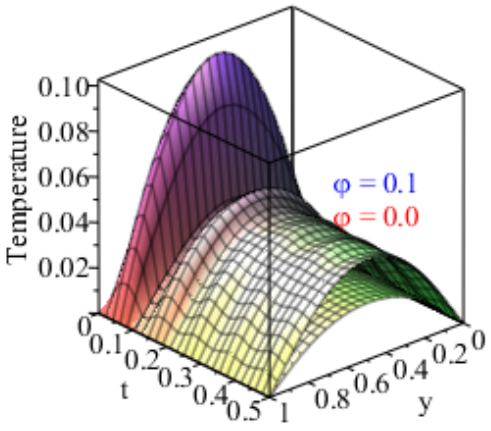

Figure 3. 3-Dimensional Display of Temperature Profile for $\varphi = 0$ and $\varphi = 0.1$

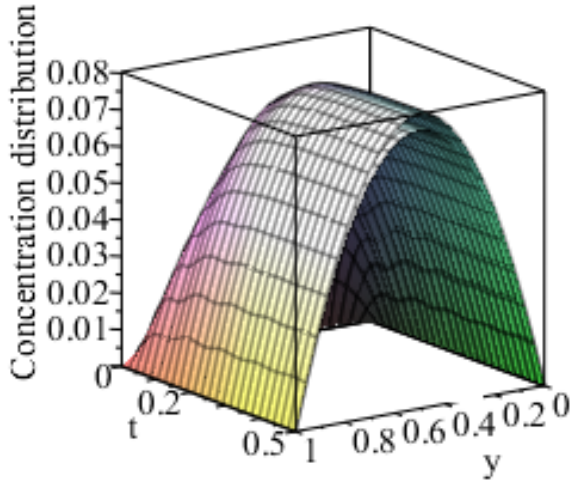

Figure 4. 3-Dimensional Display of Temperature Profile for $\varphi = 0$ and $\varphi = 0.1$

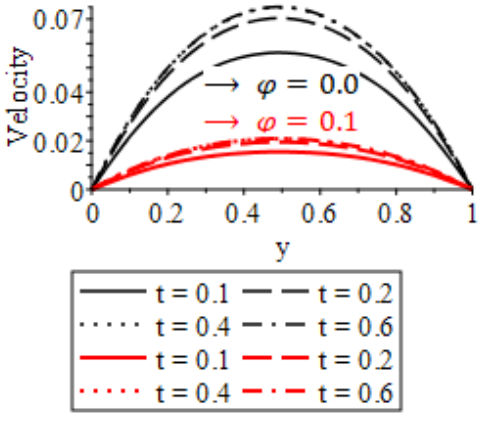

Figure 5. Variation of Time with Velocity Distribution

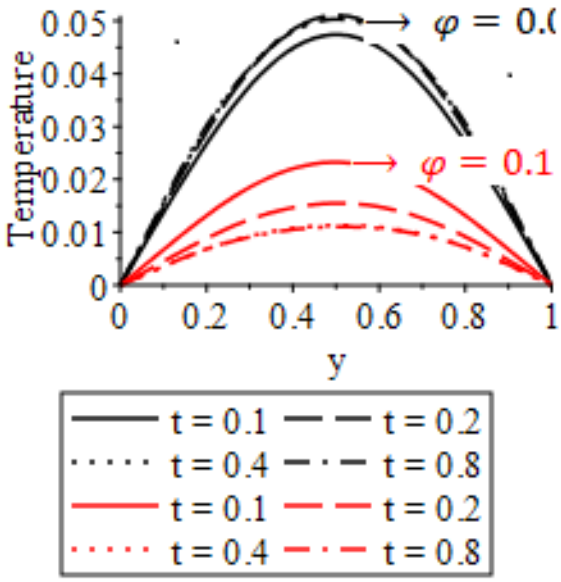

Figure 6. Variation of Time with Temperature Distribution

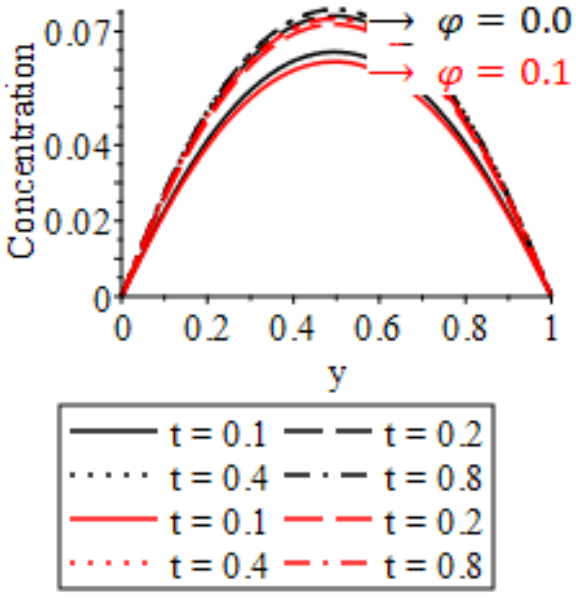

Figure 7. Variation of Time with Concentration Distribution

boundary layers. The Thermal Grashof number (Figure 8) enhances velocity through buoyancy-driven forces, increasing the overall flow rate and thickening the thermal boundary layer. Similarly, the Mass Grashof number (Figure 9) enhances fluid motion and convective mixing due to buoyancy effects from concentration gradients. The Darcy parameter (Figure 10) indicates that higher values reduce permeability and fluid velocity, leading to flatter velocity profiles and thicker boundary layers. The Dufour number (Figure 11) highlights the impact of thermal diffusion on velocity enhancement and convective mixing. Finally, binary chemical reaction parameters (Figure 12) show how reaction kinetics and buoyancy effects from heat absorption or release alter fluid properties, affecting velocity distribution and mass transport within the fluid.

Temperature Distribution

The pressure gradient in MHD nanofluid flow, influenced by the magnetic field, causes a deceleration of fluid velocity. Variable viscosity and thermal conductivity significantly affect the temperature distribution, resulting in non-uniform heat transfer. Specifically, higher thermal conductivity leads to more uniform temperature profiles, while variable viscosity impacts flow characteristics that are temperature-dependent, altering the overall behaviour of the fluid system.

The Hartmann number influences the temperature distribution within the fluid by affecting both velocity and convective heat transfer. As the Hartmann number increases, the suppression of velocity by the magnetic field reduces convective heat transfer, leading to higher temperatures near heat sources due to diminished fluid motion. This effect results in a thicker thermal boundary layer, causing less efficient heat dissipation and steeper temperature gradients near surfaces. While the core region of the flow tends to have a more uniform temperature distribution due to suppressed velocity gradients, this is counteracted by the thickened thermal boundary layer near the walls.

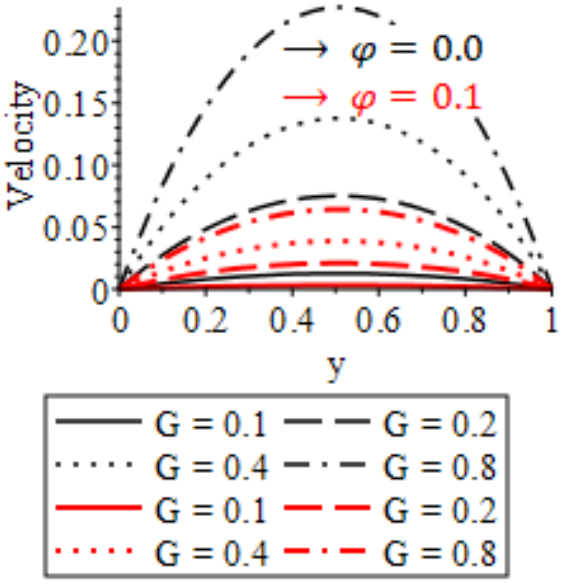

Figure 8. Impact of Pressure Gradient on Velocity Distribution

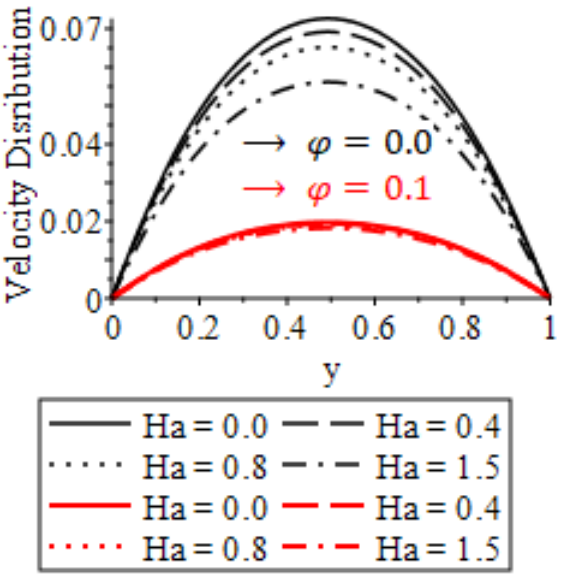

Figure 9. Impact of Hartmann Number on Velocity Distribution

The Thermal Grashof number significantly impacts the temperature distribution by enhancing buoyancy-driven convective heat transfer. Higher Grt values lead to increased temperature gradients near heated or cooled surfaces as the enhanced convection transports heat away more efficiently. Consequently, the thermal boundary layer thickness decreases, resulting in a higher heat transfer rate from the surface to the fluid. In the bulk of the fluid, away from the surface, increased convective mixing induced by higher Grt promotes a more uniform temperature distribution, reducing temperature variations and enhancing the overall efficiency of heat transfer within the system.

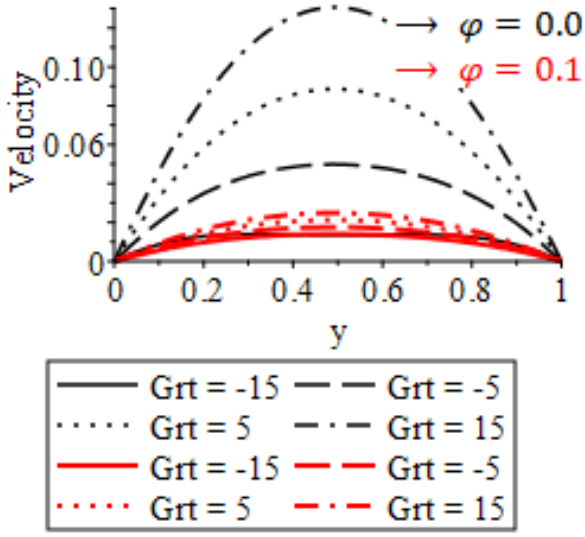

Figure 10. Influence of Thermal Grashof Number on Velocity Distribution

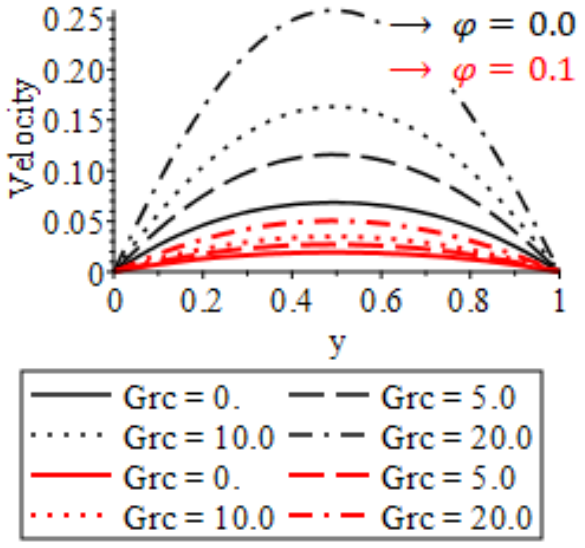

Figure 11. Influence of Mass Grashof Number on Velocity Distribution

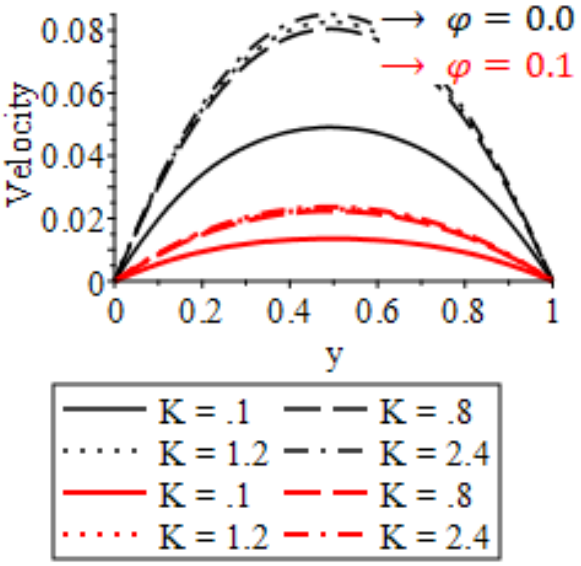

Figure 12. Effect of Porosity Parameter on Velocity Distribution

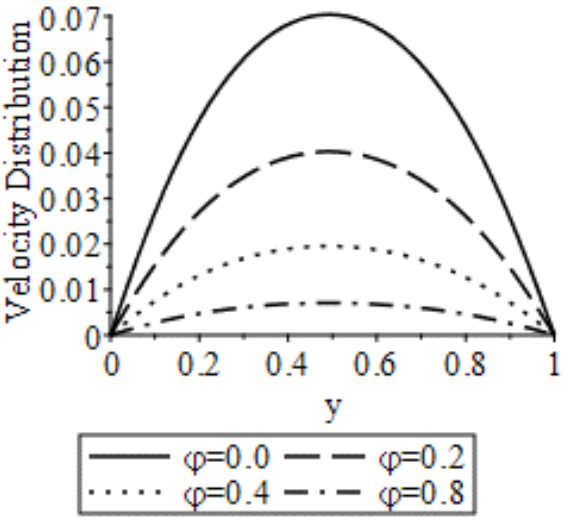

Figure 14. Influence of Introduction of Nano-Particle on Velocity Distribution

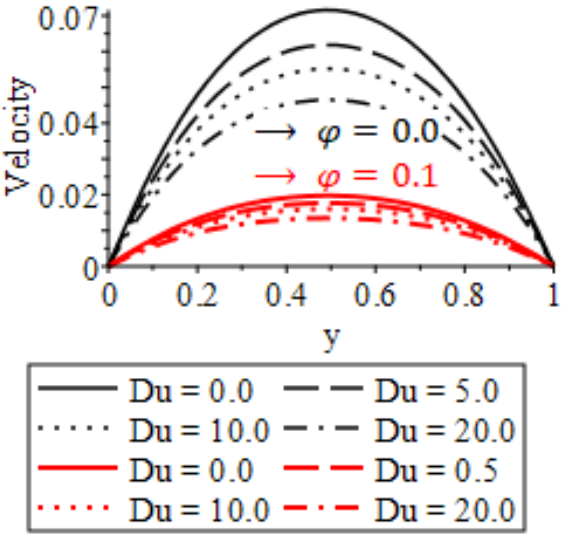

Figure 13. Influence of Dufour Number on Velocity Distribution

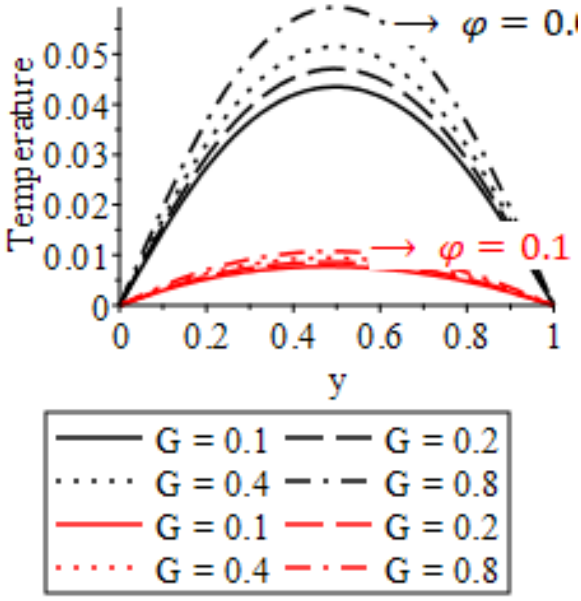

Figure 15. Effect of Pressure Gradient on Temperature Distribution

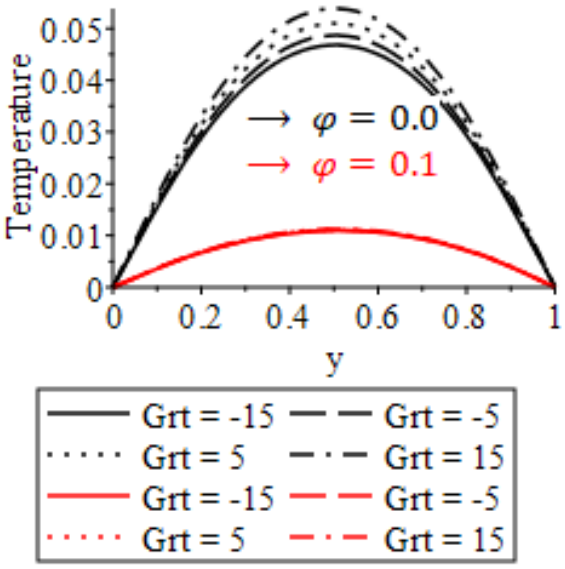

Figure 16. Influence of Thermal Buoyancy on Temperature Distribution

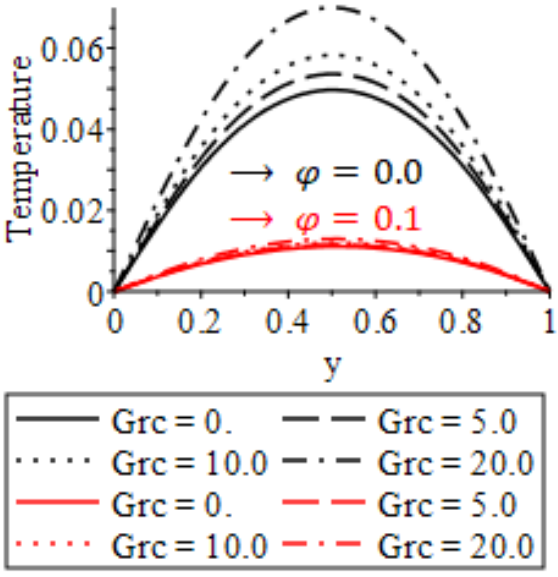

Figure 17. Effect of Mass Buoyancy on Temperature Distribution.

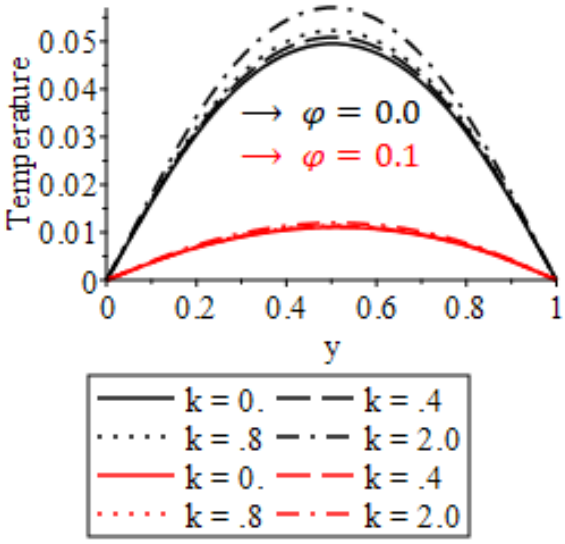

Figure 18. Effect of Temperature Dependent Viscosity on Temperature Distribution

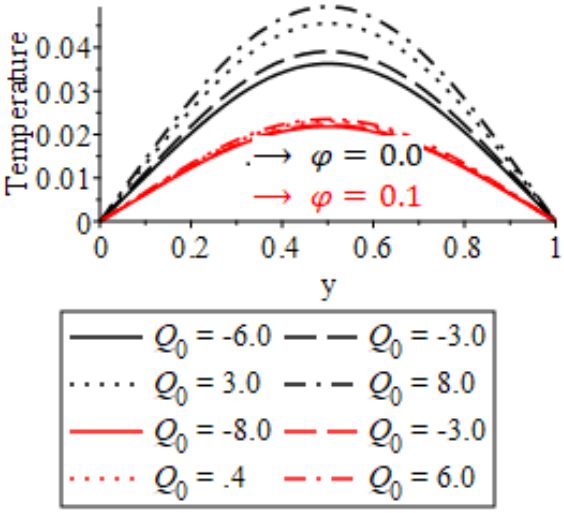

Figure 19. Contribution of Heat Generation/Absorption on Temperature Distribution

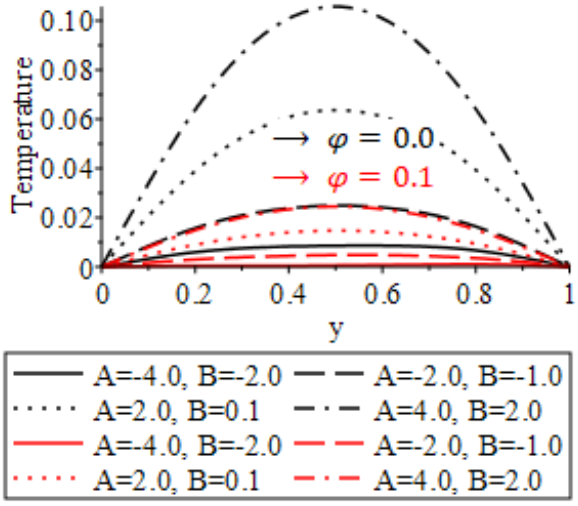

Figure 20. Influence of Time and Spatial Heat Generation on Temperature Profile

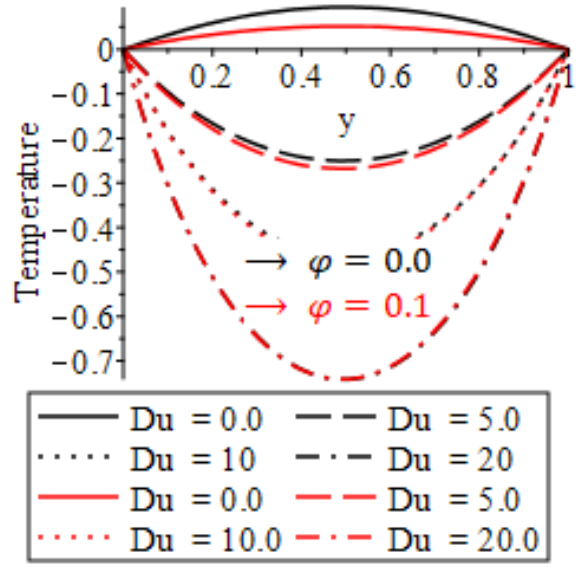

Figure 21. Effect of Dufour Number on Temperature Distribution

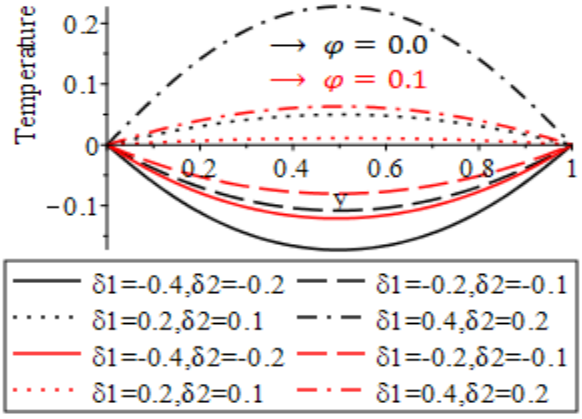

Figure 22. Effect of Binary Chemical Reaction Parameters on Temperature Distribution

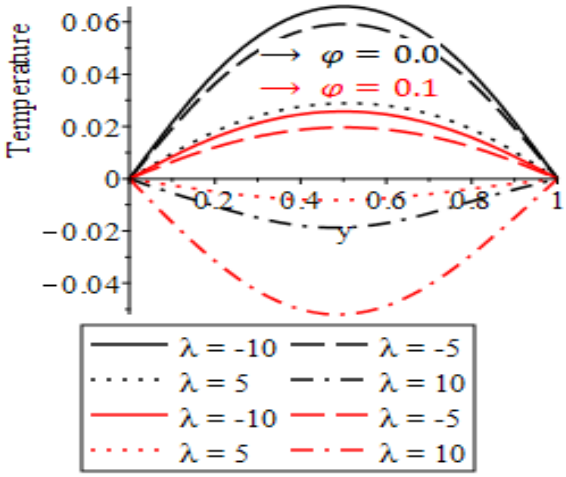

Figure 23. Influence of Reactivity Parameter on Temperature

Chemical Species Concentration

Heat generation or absorption significantly impacts fluid flow, temperature distribution, and chemical species concentration. Temperature-dependent reaction rates are influenced by heat, accelerating chemical reactions in heat-generating regions and slowing them in heat-absorbing areas. This leads to increased conversion of chemical species where temperatures are higher. Temperature gradients created by heat generation enhance buoyancy-driven mass transport, resulting in higher concentrations of chemical species in these regions. Conversely, regions of heat absorption

may experience slower mass transport and lower concentrations. Additionally, the reaction kinetics are affected, with higher temperatures favouring endothermic reactions and potentially inhibiting exothermic ones.

Binary chemical reaction parameters and the reactivity parameter play crucial roles in influencing fluid flow, temperature distribution, and chemical species concentration. Chemical reactions alter concentrations by consuming reactants and producing products, with reaction rates and stoichiometry dictating the extent of these changes. This affects mass transport, leading to non-uniform concentration profiles as products accumulate or deplete in specific regions. Higher reactivity results in faster consumption or production of chemical species, creating significant concentration gradients and faster mass transport rates. This enhances diffusion and advection processes, leading to rapid redistribution of chemical species and altered concentration profiles throughout the fluid system.

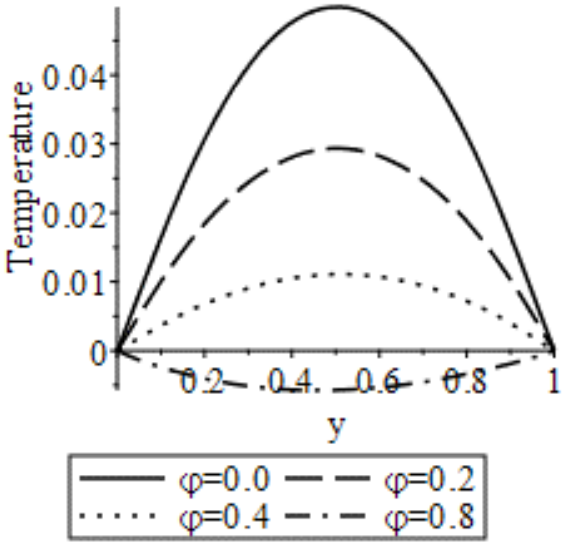

Figure 24. Effect of Nano Particle Volume Fraction on Temperature Distribution

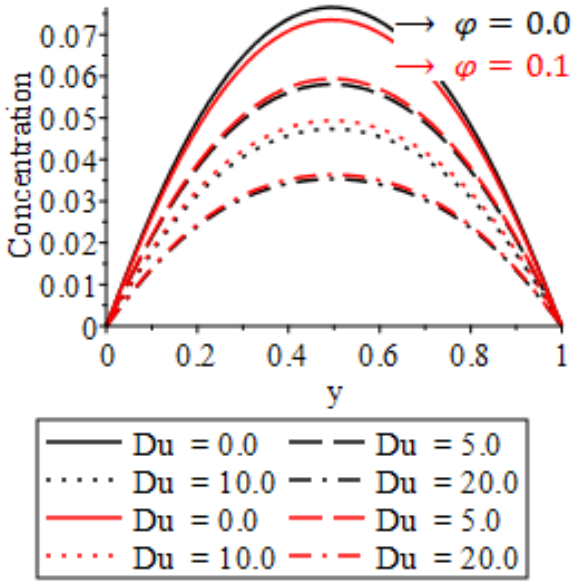

Figure 25. Influence of Dufour Number on Concentration Distribution

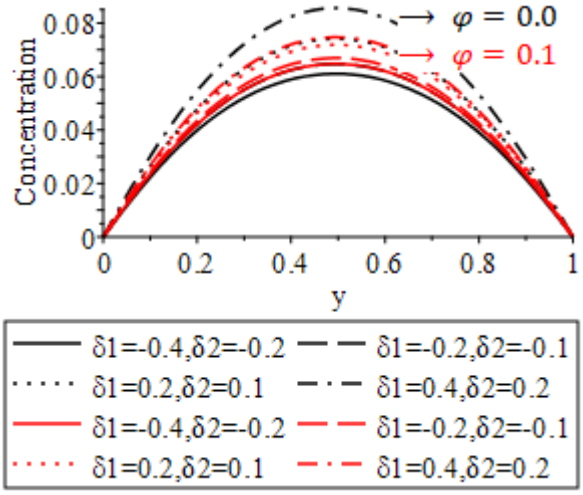

Figure 26. Influence of Binary Chemical Reaction Parameters on Concentration Distribution

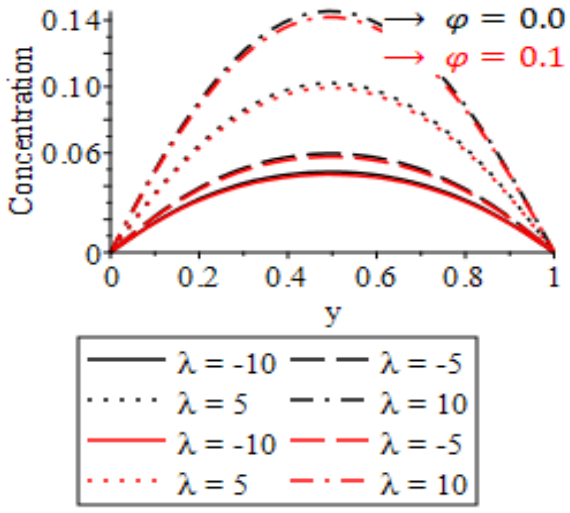

Figure 27. Effect of Reactivity Parameter on Concentration Distribution

Summary

The study of dissipative non-slip magnetohydrodynamic (MHD) nanofluid flow with variable viscosity and thermal conductivity, influenced by an Arrhenius chemical reaction, is vital for engineering and industrial applications. This research elucidates complex fluid dynamics, showing how temperature-dependent viscosity affects flow by altering viscosity gradients and boundary layer thickness, enhancing heat and mass transfer rates. Similarly, thermal conductivity, varying with nanoparticle concentration, improves heat transfer, crucial for cooling technologies and nuclear reactors. The Arrhenius chemical reaction influence's reaction rates and concentration profiles, with higher temperatures accelerating reactions and affecting thermo-physical properties like density and specific heat capacity, impacting overall flow and heat transfer. The magnetic field induces a Lorentz force, opposing fluid motion, reducing velocity, and altering thermal boundary layers, while dissipative effects like viscous dissipation and ohmic heating contribute to the energy balance. The non-slip boundary condition affects shear stress and drag force, crucial for optimizing applications such as chemical reactors and magnetic drug targeting, with future research focusing on experimental validation and sophisticated modelling.

Conclusion

In conclusion, the investigation into dissipative non-slip MHD nanofluid flow with variable viscosity and thermal conductivity in the presence of Arrhenius chemical reaction reveals several significant findings. Firstly, the presence of variable viscosity and thermal conductivity profoundly influences the velocity distributions, temperature profiles, and chemical species concentrations. The variations in these fluid properties introduce additional complexities into the flow and heat transfer phenomena, leading to non-uniform velocity and temperature fields. Moreover, the inclusion of Arrhenius chemical reaction further complicates the system dynamics, as it introduces heat generation or absorption effects, impacting both temperature and concentration gradients within the fluid domain. These findings underscore the importance of considering variable fluid properties and chemical reactions in modelling real-world nanofluid systems. Owing to the analysis presented in this current research, the following observations were made:

- Variable viscosity and thermal conductivity significantly influence velocity distributions, temperature profiles, and chemical species concentrations in MHD nanofluid flow.
- These variable fluid properties lead to non-uniform velocity and temperature fields, introducing complexities in flow and heat transfer phenomena.
- The inclusion of Arrhenius chemical reactions further complicates system dynamics by introducing heat generation or absorption effects, impacting temperature and concentration gradients.
- Parameters such as the Hartmann number, Darcy parameter, and heat generation or absorption significantly influence flow behaviour and thermal characteristics.
- The reactivity parameter is critical, dictating chemical reaction rates and affecting overall system dynamics, with higher reactivity leading to faster chemical reactions and more pronounced concentration gradients.

- Changes in viscosity due to temperature variations influence chemical species distribution and flow and temperature fields, significantly altering species concentration profiles near reactive boundaries.

- Pressure gradients affect convective heat transfer by altering the velocity field and influence viscous dissipation, contributing to local heating of the fluid.

The development of the thermal boundary layer is influenced by the pressure gradient, and regions with sharp viscosity changes due to temperature exhibit pronounced temperature gradients, impacting flow and heat transfer rates.

Contributions to Knowledge

The research significantly advances knowledge in dissipative non-slip MHD nanofluid dynamics, emphasizing variable viscosity and thermal conductivity. It illuminates the impacts of parameters like Hartmann and Dufour numbers, deepening understanding of nanofluid behaviour and thermal transport. By exploring these complexities, it enriches fundamental principles in nanofluid flow and heat transfer, offering insights into diverse conditions and chemical reactions. Additionally, it advances nanofluid engineering, addressing velocity, temperature, and chemical concentration implications, guiding optimization across engineering applications. Bridging theory with practice, it fosters innovative solutions for thermal management, energy conversion, and environmental sustainability, marking a significant contribution to the field.

Acknowledgement

Authours wish to thank the editor and the editorial team for their valuable comment which has led to improvement of this work

Conflict of Interests

The authours affirm that there is no conflict of interest.

References

Abbasi, F. M., Hayat, T. & Ahmad, B. (2015). Peristalsis of silver-water nanofluid in the presence of hall and ohmic heating effects: applications in drug deliveryю *Journal of Molecular Liquids, 207*, 248–255. http://dx.doi.org/10.1016/j.molliq.2015.03.042

Ahmed, N., Kalita, H. & Barua, D. P. (2010). Unsteady mhd free convective flow past a vertical porous plate immersed in a porous medium with hall current, thermal diffusion and heat source. *International Journal of Engineering, Science and Technology, 2*(6), 59–74. https://doi.org/10.4314/ijest.v2i6.63699

Alanazi, M., Hendi, A., Ali, B., Majeed, S., Hussein, A. & Shah, N.A. (2023). Significance of Darcy-Forchheimer Law, Activation Energy, and Brownian Motion of Tiny Particles on the Dynamics of Rotating MHD Micropolar Nanofluid. *Mathematics, 11*. https://doi.org/10.3390/math11040866

Bahiraei, M., & Hangi, M. (2015). ChemInform Abstract: Flow and Heat Transfer Characteristics of Magnetic Nanofluids: A Review. *Journal of Magnetism and Magnetic Materials, 374*, 125–138. https://doi.org/10.1016/j.jmmm.2014.08.004

Choi, S.U.S. (1995). Enhancing thermal conductivity of fluids with nanoparticles. *ASME Int. Mech. Eng. Congr. Expo., 231*, 99–105.

Dawar, A. (2018). Impact of thermal radiation and heat source/sink on eyring-powell fluid flow over an unsteady oscillatory porous stretching surface. *Math. Comput. Appl., 23*(1), 1.

Gbadeyan, J. A., Titiloye, E. O., & Adeosun, A. T. (2019). Effect of variable thermal conductivity and viscosity on Casson nanofluid flow with convective heating and velocity slip. *Heliyon, 6*(1), e03076. https://doi.org/10.1016/j.heliyon.2019.e03076

Giri, S., Das, K., & Kundu, P. (2020). Influence of nanoparticle diameter and interfacial layer on magnetohydrodynamic nanofluid flow with melting heat transfer inside rotating channel. *Mathematical Methods in the Applied Sciences. 44*. https://doi.org/10.1002/mma.6818

Hamid, Muhammad & Usman, Muhammad & Khan, Zafar & Ahmad, Rashid & Wang, Wei. (2019). Dual Solutions and Stability Analysis of Flow and Heat Transfer of Casson Fluid over a Stretching Sheet. *Physics Letters A.* https://doi.org/10.1016/j.physleta.2019.04.050

Ijaz Khan, M., Hafeez, M. U., Hayat, T., Imran Khan, M., & Alsaedi, A. (2020). Magneto rotating flow of hybrid nanofluid with entropy generation. *Computer methods and programs in biomedicine, 183,* 105093. https://doi.org/10.1016/j.cmpb.2019.105093

Jamshed, W., Ramesh, G.K., Roopa, G.S., Nisar, K.S., Safdar, R., Madhukesh, J.K., Shahzad, F., Isa, S.S., Goud, B.S., & Eid, M.R. (2022). Electromagnetic radiation and convective slippery stipulation influence in viscous second grade nanofluid through penetrable material. *ZAMM - Journal of Applied Mathematics and Mechanics / Zeitschrift für Angewandte Mathematik und Mechanik.* https://doi.org/10.1002/zamm.202200002

Jangili, S., Adesanya, S.O., Ogunseye, H.A., & Lebelo, R.S. (2018). Couple stress fluid flow with variable properties: A second law analysis. *Mathematical Methods in the Applied Sciences, 42*, 85-98. https://doi.org/10.1002/mma.5325

Lawal, M. M., Ogboru, O. K. & Okedoye, M.A. (2024). Heat and Mass Transfer Mixed Convective Electrically Conducting Nanomaterial Flow Over a Stretching Sheet. *Journal of Multidisciplinary Engineering Science and Technology, 11*(4), 16804 – 16812.

Lawal, M. M., Ogboru, O. K. & Okedoye, M.A. (2024). Influence of Electric Field Flow on MHD Nano-Fluid Over a Stretching Sheet. *American Journal of Engineering Research, 13*(4), 88-95.

Maleque, Kh. (2005). Steady Laminar Convective Flow with Variable Properties Due to a Porous Rotating Disk. *Journal of Heat Transfer-transactions of The Asme, 127.* https://doi.org/10.1115/1.2098860

Mallick, B., Misra, J. & Roy Chowdhury, A. (2019). Influence of Hall current and Joule heating on entropy generation during electrokinetically induced thermoradiative transport of nanofluids in a porous microchannel. *Applied Mathematics and Mechanics, 40,* 1509-1530. https://doi.org/10.1007/s10483-019-2528-7

Misra, S. & Kamatam, G. (2020). Effect of magnetic field, heat generation and absorption on nanofluid flow over a nonlinear stretching sheet. *Beilstein J. Nanotechnol., 11,* 976–990. https://doi.org/10.3762/bjnano.11.82

Mittal, Akhil & Kataria, Hari. (2018). Three dimensional CuO–Water nanofluid flow considering Brownian motion in presence of radiation. *Karbala International Journal of Modern Science, 4,* 275-286. https://doi.org/10.1016/j.kijoms.2018.05.002

Okedoye, A.M., Waheed, A.A., & Akinyemi, O.A. (2023). Unsteady Heat and Mass Transfer MHD Flow of Nano-Fluids with Buoyancy and Variable Thermal Conduction. *International Journal of Mathematics and Physical Sciences, 10*(2), 80-93. https://doi.org/10.5281/zenodo.7669943

Ometan, S.O., Alabi M.O. & Okedoye A.M. (2024). Analyzing the Impact of Heat and Mass Transfer on Unsteady MHD Flow with Thermal Radiation and Binary Chemical Reaction. *European Journal of Theoretical and Applied Sciences*, 2(3), 267-280. https://doi.org/10.59324/ejtas.2024.2(3).23

Osalusi, E. (2007). Effects of thermal radiation on MHD and slip flow over s porous rotating disk with variable properties. *Romanian Journal of Physics, 52*, 217-229.

Prasad, P. D., Kumar, R. K. & Varma, S. (2018). Heat and mass transfer analysis for the MHD flow of nanofluid with radiation absorption. *Ain Shams Engineering Journal,* 9, 801–813. https://doi.org/10.1016/j.asej.2016.04.016

Rashidi, F. & Nezamabad, N. M. (2011). Experimental investigation of convective heat transfer coefcient of cnts nanofluid under constant heat flux. *Proc. World Cong. Eng.,* 3, 1618–1624.

Saeed, A., Alghamdi, W., Mukhtar, S., Shah, S. I. A., Kumam, P., Gul, T., Nasir, S., & Kumam, W.

(2021). Darcy-Forchheimer hybrid nanofluid flow over a stretching curved surface with heat and mass transfer. *PloS one, 16*(5), e0249434. https://doi.org/10.1371/journal.pone.0249434

Savvas T.A., Marktos N.C., & Papaspyrides C.D. (1994). On the flow of non-Newtonian polymer solution. *Appl. Math. Model. 1994*; 18, 14–22.

Shah, Z., Dawar, A., Kumam, P., Khan, W.N., & Islam, S. (2019). Impact of Nonlinear Thermal Radiation on MHD Nanofluid Thin Film Flow over a Horizontally Rotating Disk. *Applied Sciences.* 9, 1533. https://doi.org/10.3390/APP9081533

Sheikholeslami, M. (2019). Numerical approach for mhd al2o3-water nanofluid transportation inside a permeable medium using innovative computer method. *Computational Methods in Applied Mechanics and Engineering, 344*, 306–318. https://doi.org/10.1016/J.CMA.2018.09.042

Singh, A. K. (2003). Numerical solution of hydromagnetic unsteady free convection flow past an infnite porous plate. *Indian Journal of Pure and Applied Physics, 41*, 167–170

Singh, P., Roy, S. & Pop, I. (2008). Unsteady mixed convection from a rotating vertical slender cylinder in an axial flow. *International Journal of Heat and Mass Transfer, 51,* 1423-1430. https://doi.org/10.1016/j.ijheatmasstransfer.2007.11.024

Tania, S. K. & Samad, M. A. (2010). Effects of radiation, heat generation and viscous dissipation on mhd free convection flow along a stretching sheet. *Research Journal of Applied Sciences, Engineering and Technology, 2*(4), 368–377.

Tufail, M., Saleem, M., & Chaudhry, Q. (2020). Heat Transfer Analysis For The Unsteady Ucm Fluid Flow With Hall Effects: The Two-Parameter Lie Transformations. *Frontiers In Heat And Mass Transfer, 15,* 14. https://doi.org/10.5098/Hmt.15.14

Umavathi, J.C., Chamkha, A.J., & Mohiuddin, S.M. (2015). Combined effect of variable viscosity and thermal conductivity on free convection flow of a viscous fluid in a vertical channel using DTM. *Meccanica, 51*, 71 - 86. https://doi.org/10.1007/s11012-015-0202-4

Vincent, B., Kang'ethe, G., & Kiogora, P.R. (2020). Analysis of Magnetohydrodynamics Flow of Incompressible Fluids over Oscillating Bottom Surface with Heat and Mass Transfer. *International Journal of Mathematics and Mathematical Sciences, 2020,* 1-12. https://doi.org/10.1155/2020/4054578

Waini, I., Khashi'ie, N. S., Kasim, A. R. M., Zainal, N. A., Hamzah, K. B., Md Arifn, N. & Pop, I. (2022). Unsteady magnetohydrodynamics (MHD) flow of hybrid ferrofluid due to a rotating disk. *Mathematics, 10*(10), 1658. https://doi.org/10.3390/math10101658